

Modulation of Agostic B–H→Ru Bonds in *exo*-Monophosphino-7,8-Dicarba-*nido*-undecaborate Derivatives

Clara Viñas,^{*,†} Rosario Nuñez,[†] Francesc Teixidor,[†] Raikko Kivekäs,[‡] and Reijo Sillanpää[§]

Institut de Ciència de Materials de Barcelona, CSIC, Campus de Bellaterra, Cerdanyola, 08193 Barcelona, Spain, Inorganic Chemistry Laboratory, Box 55, University of Helsinki, FIN-00014 Helsinki, Finland, and Department of Chemistry, University of Turku, FIN-20500 Turku, Finland

Received November 22, 1995[⊗]

The series of compounds [7-PPh₂-8-R-7,8-C₂B₉H₁₀]⁻ behaves as tricoordinating ligands toward Ru(II). The coordination takes place by means of the *exo*-cluster PPh₂ group and boron atoms B(2) and B(11) through B–H→Ru agostic bonds. The three remaining Ru(II) positions may be occupied by two equivalent or distinct neutral ancillary ligands and one coordinating anion. The ¹H NMR spectra of these complexes provide evidence for the participation of two B–H's in bonding to Ru(II). A resonance near -3 ppm is indicative of a B–H→Ru agostic bond with a large contribution of B–H, while a resonance close to -15 ppm is indicative of a B–H→Ru agostic bond with a large contribution of Ru–H. A gradation of agostic bonds with intermediate situations may be produced. These have been achieved by synthesizing a series of complexes [RuX(7-PPh₂-8-R-C₂B₉H₁₀)LL'], where X = Cl or H, R = H, Me, or Ph, L = PPh₃, and L' = PPh₃, CO, tetrahydrothiophene, or ethanol. Combinations have been done. The study has shown that the nature of R at the 8-cluster position practically has little effect on the B–H→Ru resonance; however, the nature of the *trans* ancillary ligand is highly perturbing. The effect has been compared to the *trans* influence. The study has permitted evaluation of the *trans* influence (*I*) of a series of ligands. The order *I*(H) > *I*(PR₃) > *I*(CO) > *I*(BH) > *I*(Cl) is followed. An NMR quantitative figure of this *trans* influence is given; however, due to the limited number of complexes tested it must be taken as only of qualitative value. The structural assignments are supported by the molecular structures of [RuCl(7-PPh₂-8-Me-7,8-C₂B₉H₁₀)(PPh₃)₂] (**1**) and [RuCl(7-PPh₂-8-Me-7,8-C₂B₉H₁₀)(EtOH)(PPh₃)₂]·0.64 (Me)₂CO (**2**).

Introduction

We have recently described how the groups B(2)–H and B(11)–H in [7,8-C₂B₉H₁₂]⁻ derivatives can be forced to participate in bonding to a metal through B(2)–H→Ru and B(11)–H→Ru agostic bonds.¹ The existence of a single PR'₂ coordinating group in the carborane molecule [7-PPh₂-8-R-C₂B₉H₁₀]⁻ requires two appropriate BH entities to participate in coordination and render the ligand tridentate. Though B–H→M coordination in [7,8-C₂B₉H₁₂]⁻ derivatives has been known for many years, mainly in *exo-nido* species² or in dimetal species of which [Ni₂(CO)₂(η⁵-7,8-Me₂-7,8-C₂B₉H₉)₂] is a recent example,³ the participation of B(3)–H→M⁴ and B(2)–H→M and B(11)–H→M has just been recently reported.¹ On the other hand, the control of spectroscopic properties or the reactivity of complexes by modification of the nature of the ancillary ligands is a subject of current interest. Recently, Li and Taube^{5,6} described how the spectroscopic properties of the complexes *trans*-[Os(H···D)X(en)₂]⁺ and *trans*-[Os(H···D)X(NH₃)₄]⁺ change

substantially as the *trans* ligand is varied. There is also evidence that the isomer of [Ir(H···H)(H)Cl₂(PⁱPR₃)₂] with H₂ *trans* to Cl is more stable with respect to H₂ loss than the one with H₂ *trans* to H.⁷ In *trans*-

(2) (a) Baker, R. T.; King, R. E.; Knobler, C.; O'Con, C. A.; Hawthorne, M. F. *J. Am. Chem. Soc.* **1978**, *100*, 8266. (b) Long, J. A.; Marder, T. B.; Behnken, P. E.; Hawthorne, M. F. *J. Am. Chem. Soc.* **1984**, *106*, 2979. (c) Knobler, C. B.; Marder, T. B.; Mizusawa, E. A.; Teller, R. G.; Long, J. A.; Behnker, P. E.; Hawthorne, M. F. *J. Am. Chem. Soc.* **1984**, *106*, 2990. (d) Long, J. A.; Marder, T. B.; Hawthorne, M. F. *J. Am. Chem. Soc.* **1984**, *106*, 3004. (e) Behnken, P. E.; Belmont, J. A.; Busby, D. C.; Delaney, M. S.; King, R. E., III; Kreimendahl, C. W.; Marder, T. B.; Wilczynski, J. J.; Hawthorne, M. F. *J. Am. Chem. Soc.* **1984**, *106*, 3011. (f) Behnken, P. E.; Busby, D. C.; Delaney, M. S.; King, R. E., III; Kreimendahl, C. W.; Marder, T. B.; Wilczynski, J. J.; Hawthorne, M. F. *J. Am. Chem. Soc.* **1984**, *106*, 7444. (g) Behnken, P. E.; Marder, T. B.; Baker, R. T.; Knobler, C. B.; Thompson, M. R.; Hawthorne, M. F. *J. Am. Chem. Soc.* **1985**, *107*, 932. (h) Belmont, J. A.; Soto, J.; King, R. E., III; Donaldson, A. J.; Hewes, J. D.; Hawthorne, M. F. *J. Am. Chem. Soc.* **1989**, *111*, 7475. (i) Green, M.; Howard, J. A. K.; Jelfs, A. N. de M.; Johnson, O.; Stone, F. G. A. *J. Chem. Soc., Dalton Trans.* **1987**, 73. (j) Khasnis, D. V.; Toupet, L.; Dixneuf, P. H. *J. Chem. Soc., Chem. Commun.* **1987**, 230. (k) Crowther, D. J.; Baenziger, N. C.; Jordan, R. F. *J. Am. Chem. Soc.* **1991**, *113*, 1455.

(3) (a) Carr, N.; Mullica, D. F.; Sappenfield, E. L.; Stone, F. G. A. *Inorg. Chem.* **1994**, *33*, 1666. (b) Baker, R. T.; Calabrese, J. C.; Westcott, S. A.; Nguyen, P.; Marder, T. B. *J. Am. Chem. Soc.* **1993**, *115*, 4367. (c) Baker, R. T.; Calabrese, J. C.; Westcott, S. A.; Marder, T. B. *J. Am. Chem. Soc.* **1995**, *117*, 8777. (d) Hartwig, J. F.; Bhandari, S.; Rablen, P. R. *J. Am. Chem. Soc.* **1994**, *116*, 1839.

(4) Teixidor, F.; Ayllón, J. A.; Viñas, C.; Kivekäs, R.; Sillanpää, R. *Organometallics* **1994**, *13*, 2751.

(5) (a) Li, Z.; Taube, H. *J. Am. Chem. Soc.* **1991**, *113*, 8946. (b) Hasegawa, T.; Li, Z.; Parking, S.; Hope, H.; McMullan, R. K.; Koetzle, T. F.; Taube, H. *J. Am. Chem. Soc.* **1994**, *116*, 4352.

(6) Li, Z.; Taube, H. *Science* **1992**, *256*, 210.

[†] Institut de Ciència de Materials de Barcelona.

[‡] University of Helsinki. Present address: Department of Chemistry, Universitat Autònoma de Barcelona, Campus de Bellaterra, Cerdanyola, 08193 Barcelona, Spain.

[§] University of Turku.

[⊗] Abstract published in *Advance ACS Abstracts*, August 1, 1996.

(1) Teixidor, F.; Viñas, C.; Nuñez, R.; Flores, M. A.; Kivekäs, R.; Sillanpää, R. *Organometallics* **1995**, *14*, 3952.

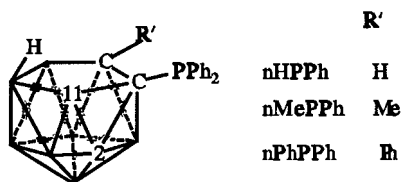


Figure 1. Schematic drawing of monophosphine derivatives of 7,8-dicarba-*nido*-undecaborate(1⁻).

[Ru(H₂)H(PR₂CH₂CH₂PR₂)₂]⁺, the structure and acidity of the compound change with a systematic change in *cis* bidentate phosphine ligands⁸ or by modifying the X nature (X = H, Cl) in *trans*-[Ru(H₂)X(PR₂CH₂CH₂PR₂)₂]⁺.⁹ We have proven that the strength of the B(3)–H→Ru bond could be modulated in a series of [RuCl(7,8-SRS-C₂B₉H₁₀)(PPh₃)₂] compounds by modifying the length of the S–R–S spacer.⁴ To modulate the strength of the B(2)–H→Ru and B(11)–H→Ru linkages in Ru complexes of [7-PPh₂-8-R-C₂B₉H₁₀]⁻, there were two possibilities: modification of the cluster 8-R group or modification of the ancillary ligands. We report here the preparation of the complexes [RuX(7-PPh₂-8-R-C₂B₉H₁₀LL') to learn more about the factors governing the strength and spectroscopic properties of the B–H→Ru agostic bonds.

Results and Discussion

Monophosphines of the type indicated in Figure 1 have been proven to be tridentate when they are bonded to Ru(II), which is an octahedrally demanding transition metal ion.¹ The coordination takes place by means of the cluster PPh₂ group and boron atoms B(2) and B(11) through B–H→Ru agostic bonds. The monophosphine species offer the possibility of being separated into enantiomers and consequently being used as tricoordinating [P, BH(2), BH(11)] or dicoordinating [P, BH(11)] anionic chiral ligands in asymmetric catalysis.

Throughout the text the ligand [7-PPh₂-8-R-7,8-C₂B₉H₁₀]⁻ will be abbreviated as [nRPPh]⁻, where n represents the moiety [7,8-C₂B₉H₁₀]⁻, PPh the PPh₂ group connected to C(7), and R the organic radical bonded to C(8). The abbreviations [nMePPh]⁻, [nPhPPh]⁻, and [nHPPh]⁻ are used for R = Me, Ph, and H, respectively.

The reaction of [nMePPh]⁻ with [RuCl₂(PPh₃)₃] in a 1:1 ratio in ethanol produced an orange solid with the stoichiometry [RuCl(nMePPh)(PPh₃)₂] (**1**). This stoichiometry suggests that the ligand [nMePPh]⁻ bonds in a tricoordinating way, which might take place via the *exo*-cluster PPh₂ unit and two BH groups. The ¹H NMR spectrum displays broad signals at –14.90 and –3.42 ppm, which are assigned to two sorts of B–H→Ru agostic bonds. This diversity of B–H→Ru chemical shifts is noticeable and is the largest that we have encountered in related compounds.

We reported earlier⁴ that the agostic B(3)–H→Ru bonds could be dealt with as a compromise between two extreme situations, A and B motifs, which are shown

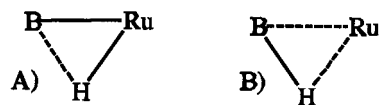


Figure 2. Proposed molecular structures for forms A and B related to agostic B–H→Ru bonds.

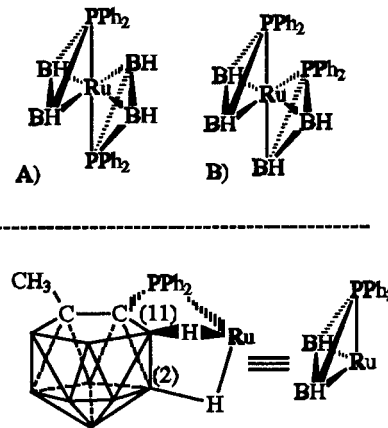


Figure 3. Isomers compatible with the formulation [Ru-(nMePPh)₂]. The equivalence simplification that represents the 7-(diphenylphosphine)-8-methyl-7,8-dicarba-*nido*-undecaborate anion is at the bottom.

in Figure 2. If we extend this to B–H→Ru bonds other than B(3)–H→Ru, we may conclude that in **1** the resonance at –14.90 ppm has a larger A contribution while the one at –3.42 ppm has a larger B contribution.

The ¹H{¹¹B} NMR spectrum of **1** reveals that the broad resonance at –3.42 ppm is in fact a doublet with ²J(H,P) = 38 Hz, which is assigned to a BH *trans* to a PPh₃ ligand. The resonance at –14.90 ppm is a singlet. The chemical shift dispersion of these B–H→Ru ¹H NMR resonances was controversial since it could be due to the BH cluster site disposition or to the PR₃ *trans* influence. To discern which of these two factors is relevant, we will discuss the spectra of *trans*- and *cis*-[Ru(nMePPh)₂] that were reported earlier.¹ In *trans*-[Ru(nMePPh)₂] (Figure 3A), the two *exo*-cluster PPh₂ groups are in a *trans* arrangement, so that each BH participating in a B–H→Ru bond has another BH *trans* to it. Under those circumstances, no phosphorus *trans* influence was possible on any BH. The B(2)–H→Ru and B(11)–H→Ru resonances in *trans*-[Ru(nMePPh)₂] appear at –11.20 and –10.32 ppm, showing little cluster site dependence of the B–H→Ru resonance. In *cis*-[Ru(nMePPh)₂] (Figure 3B) where the B(2)–H is *trans* to the *exo*-cluster PPh₂ group, two B–H→Ru resonances, one at –5.55 and the other at –10.70 ppm, have been found. The high-field resonance has a δ value close to those found in *trans*-[Ru(nMePPh)₂], –10.70 vs –11.20 or –10.32 ppm, but the second B–H→Ru resonance has experienced a downfield shift caused by the *exo*-cluster PPh₂, which is *trans* to the B(2)–H. Consequently, we have arrived at the fact that the B–H→Ru chemical shift is due to the ancillary ligand *trans* to it and not to the BH site in the cluster.

Taking into account the two B–H→Ru resonances in **1** at –14.90 and –3.42 ppm, the former discussion confirms that only one of the B–H's involved in B–H→Ru bonding is *trans* to a PPh₃. Three isomers are compatible with the [RuCl(nMePPh)(PPh₃)₂] (**1**) stoichiometry, which are indicated schematically in Figure 4 as motifs A, B, and C. In these, only a fragment of the cluster is drawn. The *all-cis* motif B

(7) Albinati, A.; Bakhmutov, V. I.; Caulton, K. G.; Clot, E.; Eckert, J.; Eisenstein, O.; Gusev, D. G.; Grushin, V. V.; Hauger, B. E.; Klooster, W. T.; Koetzle, T. F.; McMullan, R. K.; O'Loughlin, T. J.; Pelissier, M.; Ricci, R. S.; Sigalas, M. P.; Vymenits, A. B. *J. Am. Chem. Soc.* **1993**, *115*, 7300.

(8) Cappellani, E. P.; Drouin, S. D.; Jia, G.; Maltby, P. A.; Morris, R. H.; Schweitzer, C. T. *J. Am. Chem. Soc.* **1994**, *116*, 3375.

(9) Chin, B.; Lough, A. J.; Morris, R. H.; Schweitzer, C. T.; D'Agostino, C. *Inorg. Chem.* **1994**, *33*, 6278.

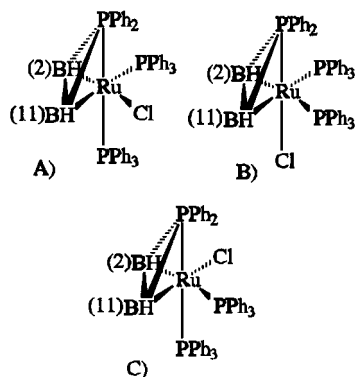


Figure 4. Isomers compatible with the formulation $[\text{RuCl}(\text{nRPPh})(\text{PPh}_3)_2]$.

distribution is excluded due to the large $^2J(\text{P},\text{P})$ coupling constant found in the $^{31}\text{P}\{^1\text{H}\}$ NMR of **1**, [$^2J(\text{P},\text{P})_t = 294$ Hz], which is an indication of a *trans*-P-P disposition in the complex.¹⁰ This is in agreement with only one BH group *trans* to a PPh_3 . The A and C motifs are difficult to distinguish since both have a quite similar chromophore: B-H *trans* to Cl, *exo*-cluster PPh_2 *trans* to PPh_3 , and B-H *trans* to PPh_3 . These A and C motifs provide information about the high-field resonance at -14.90 ppm in **1**, which is at higher field than in *trans*- $[\text{Ru}(\text{nMePPh})_2]$. In A and C (Figure 4), one BH has a *trans*- PPh_3 and the second BH has a Cl. Then we may use the following hypothesis: replacement of the *trans*-BH by $\text{PR}'\text{R}''_2$ shifts its *trans*-B-H-Ru resonance downfield (in **1** to -3.42 ppm), and replacement of the *trans*-BH by a Cl shifts its *trans*-B-H-Ru resonance upfield (in **1** to -14.90 ppm). A BH *trans* to a second BH has been taken as a reference point, as in *trans*- $[\text{Ru}(\text{nMePPh})_2]$. To confirm and extend this hypothesis, other compounds of the series $[\text{RuCl}(\text{nMePPh})(\text{L})(\text{PPh}_3)]$, $[\text{RuCl}(\text{nRPPh})(\text{PPh}_3)_2]$, and $[\text{RuH}(\text{nRPPh})(\text{PPh}_3)_2]$ are synthesized.

The $[\text{RuCl}(\text{nMePPh})(\text{L})(\text{PPh}_3)]$ Series. This series is intended to produce complexes with different ancillary ligands, *cis* or *trans* to B-H's participating in B-H-Ru bonds.

Compound **1** dissolves in a mixture of chloroform, EtOH, and acetone, forming, in the presence of O_2 , a new species $[\text{RuCl}(\text{nMePPh})(\text{EtOH})(\text{PPh}_3)]$ (**2**) (Figure 5). The process was followed by $^{31}\text{P}\{^1\text{H}\}$ NMR. The three resonances of **1** diminish while signals at 36.40 [$^2J(\text{P},\text{P})_c = 42$ Hz], 68.08 [$^2J(\text{P},\text{P})_c = 42$ Hz], and 29.97 ppm appear. The resonance at 29.97 ppm is characteristic of Ph_3PO while the other two are related to the new compound **2**. In the absence of oxygen, the reaction does not take place. Compound **2** was isolated as pure red crystals from this solution.

The ^1H NMR spectrum of **2** displays two wide resonances, one at -15.01 ppm and the second at -1.06 ppm. These are relatively similar to those found in the ^1H NMR spectrum of **1**, which suggest that a PPh_3 group *trans* to BH is preserved in **2**. In addition, the $^{11}\text{B}\{^1\text{H}\}$ NMR spectrum displays a pattern comparable to that of **1** and the $^2J(\text{P},\text{P})$ observed in the $^{31}\text{P}\{^1\text{H}\}$ NMR spectrum, 42 Hz, implies that the *exo*-cluster PPh_2 and PPh_3 units are in a *cis* disposition. Thus, in the process

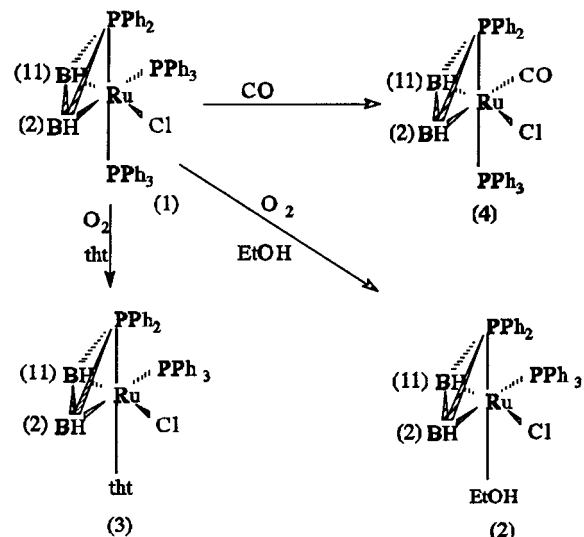


Figure 5. Schematic reactions of $[\text{RuCl}(\text{nMePPh})(\text{PPh}_3)_2]$ (**1**).

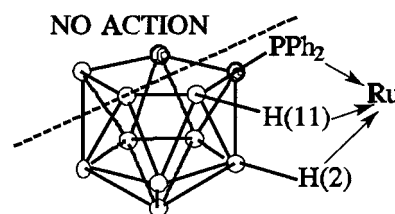


Figure 6. Diagram showing the nonactive and active parts of the cluster.

to form **2** (Figure 5), the leaving group must be *trans* to the *exo*-cluster PPh_2 , invoking a *trans* effect. The proposed structure is indicated in Figure 5.

A similar reaction was carried out with tetrahydrothiophene (tht) to obtain compound $[\text{RuCl}(\text{nMePPh})(\text{tht})(\text{PPh}_3)]$ (**3**). The spectroscopic properties were similar to those of **2**. The result was a compound similar to **2** where the ethanol molecule has been replaced by tht.

Neither **2** nor **3** provides additional information on the *trans* influence on B-H-Ru resonances since the ancillary ligands, EtOH and tht, are placed *cis* to the BH groups. They prove, however, that in the first instance it is reasonable to reject the *cis* influence.

The reaction of **1** with CO provides an alternative way of eliminating one PPh_3 group. The bubbling of CO through a chloroform solution of **1** provides $[\text{RuCl}(\text{nMePPh})(\text{CO})(\text{PPh}_3)]$ (**4**), whose $^{31}\text{P}\{^1\text{H}\}$ NMR spectrum shows two resonances, one at -7.47 ppm [$^2J(\text{P},\text{P})_t = 236$ Hz], and the other one at 24.28 ppm [$^2J(\text{P},\text{P})_t = 236$ Hz]. This large $^2J(\text{P},\text{P})$ value indicates that the P atoms are in a *trans* arrangement. Schematically the reaction is described in Figure 5. In compound **4** the CO is *trans* to a BH participating in a B-H-Ru bond.

The $[\text{RuCl}(\text{nRPPh})(\text{PPh}_3)_2]$ Series. This series is intended to produce complexes with different groups on C(8) while keeping the ancillary ligands constant. In metal complexes of $[\text{nMePPh}]^-$ and similar ligands, bonding takes place preferentially on one side of the ligand, with the second half remaining inactive. This is depicted in Figure 6. Thus, it has been possible to activate, by Ru complexation, two otherwise inactive B(2) and B(11) boron atoms just by using a monodentate coordinating group. In $[\text{7,8-SRS-7,8-C}_2\text{B}_9\text{H}_{10}]^-$ derivatives (see Figure 7) modulation of the B(3)-H-M bond

(10) (a) Verkade, J. G.; Quin L. D. *Phosphorus-31 NMR Spectroscopy in Stereochemical Analysis: Organic Compounds and Metal Complexes*; Marchand, A. P.; Denton, TX, 1987. (b) Verkade, J. G.; Quin L. D. *Phosphorus-31 NMR Spectral Properties in Compound Characterization and Structural Analysis*; VCH Publishers: New York, 1994.

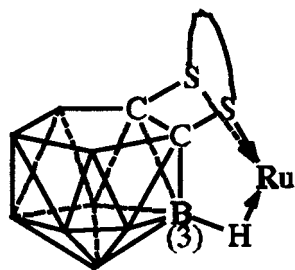
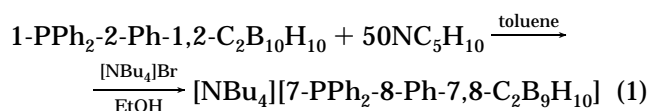


Figure 7. Formation of the B(3)–H→Ru agostic bond in [7,8-SRS-7,8-C₂B₉H₁₀][−] derivatives.

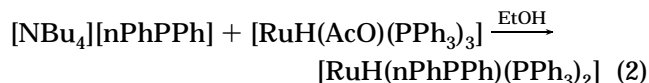
strength was possible by varying the length of the SRS spacer, an intrinsic component of the ligands.⁴ A similar modulating B–H→Ru effect in compounds such as **1** by the variation of the bulkiness and nature of the group bonded to C(8) was examined. To do so, the ligands [7-PPh₂-7,8-C₂B₉H₁₀][−], [nHPPh][−] and [7-PPh₂-8-Ph-7,8-C₂B₉H₁₀][−], [nPhPPh][−] have been synthesized. See eq 1 for [nPhPPh][−].



A similar preparation procedure described earlier for the synthesis of **1** has led to [RuCl(nHPPh)(PPh₃)₂] (**5**) and [RuCl(nPhPPh)(PPh₃)₂] (**6**), which behave toward O₂ in the same manner as **1**. The ³¹P{¹H} NMR and ¹¹B{¹H} NMR spectra of these compounds are comparable to those of **1**, as shown in the Experimental Section. The spectral similarity suggests that the structures are similar to that indicated earlier for **1** (Figure 5).

The ¹H NMR spectrum of **5** displays broad signals at −14.90 and −3.50 ppm, which again are assigned to two different types of B–H→Ru agostic bonds. We have used this compound to perform the assignment of the resonances to specific boron and hydrogen atoms of the cluster. A partial assignment of the ¹¹B{¹H} NMR resonances of **5** has been possible by a COSY ¹¹B{¹H}/¹¹B{¹H} 2D NMR experiment, which establishes the following correspondences (ppm): 5.67 (B(6)), −16.50 (two boron atoms), −17.57 (B(11)), −19.19 (two boron atoms), −27.38 (B(10)), −30.32 (B(2)), −36.67 (B(1)). On the other hand, HETCOR ¹¹B/¹H 2D NMR (see Figure 8) shows that the resonance at −3.50 ppm is due to B(2)–H→Ru and that at −14.90 ppm is due to B(11)–H→Ru. Furthermore, the resonance at −3.50 ppm is a doublet in the ¹H{¹¹B} NMR spectrum, which indicates that a PPh₃ group exists in the *trans* position for B(2). Thus, the isomer C shown in Figure 4 is obtained.

The [RuH(nRPPh)(PPh₃)₂] Series. To estimate the H[−] *trans* influence on B–H→Ru, the complexes [RuH(nMePPh)(PPh₃)₂] (**7**), [RuH(nHPPh)(PPh₃)₂] (**8**), and [RuH(nPhPPh)(PPh₃)₂] (**9**) were synthesized following eq 2, which illustrates **9**.



Compounds, **7–9** are similar, so we will center our discussion on only one.

The ¹H NMR spectrum of **9** displays broad signals at −13.90 (RuH), −6.75 (BHRu), and −2.40 ppm (BHB) and a tetraplet at −1.80 ppm [¹J(H,B) = 105 Hz]

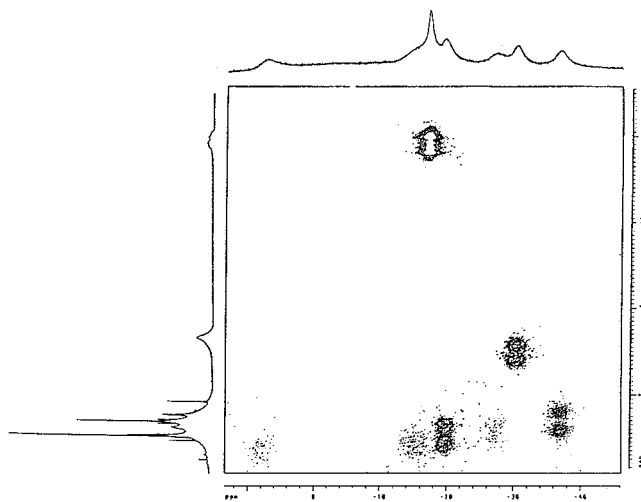


Figure 8. Heteronuclear correlation ¹¹B/¹H 2D NMR of [RuCl(nHPPh)(PPh₃)₂] (**5**).

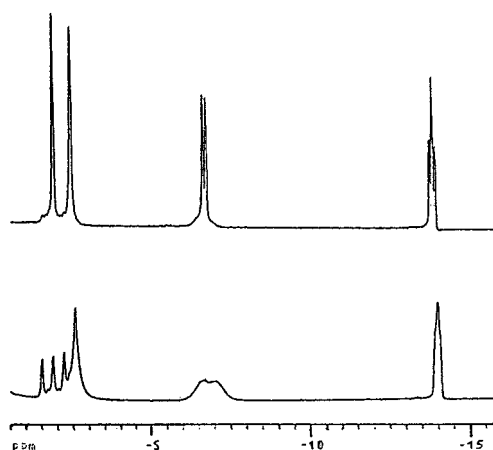


Figure 9. High-field regions of ¹H{¹¹B} and ¹H NMR spectra of [RuH(nPhPPh)(PPh₃)₂] (**9**).

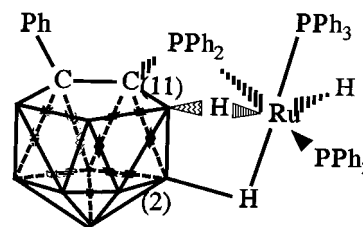


Figure 10. Proposed structure for [RuH(nPhPPh)(PPh₃)₂] (**9**).

(BHRu). Its ¹H{¹¹B} NMR spectrum reveals that the broad resonance at −6.75 is, in fact, a doublet [²J(H,P) = 30 Hz], assigned to a BH *trans* to an ancillary ligand PPh₃. The hydride portions of the ¹H NMR and ¹H{¹¹B} NMR spectra of **9** are displayed in Figure 9.

The ³¹P{¹H} NMR spectrum is in agreement with either isomer A or C in Figure 4. The ¹¹B{¹H} NMR spectrum is almost indistinguishable from those found in the Cl[−] series; consequently, the boron assignments to specific resonances are kept. On this basis, HETCOR ¹¹B/¹H 2D NMR proves that the ¹H NMR tetraplet at −1.80 ppm is due to the B(11)H, thus proving that the observed isomer is C, the same as that for the Cl[−] series. The proposed structure for **9** is presented in Figure 10.

Crystal Structures of [RuCl(nMePPh)(PPh₃)₂] (1**) and [RuCl(nMePPh)(EtOH)(PPh₃)₂]-0.64(Me)₂CO (**2**).** Up to now most of this discussion has been based on NMR techniques. To confirm some of the proposed

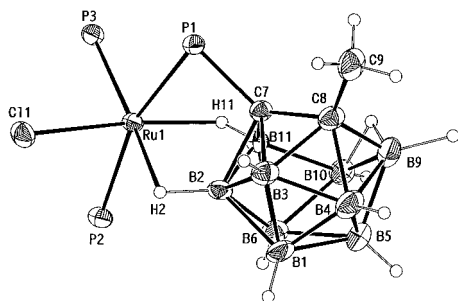


Figure 11. Simplified ORTEP view of $[\text{RuCl}(\text{nMePPh})(\text{PPh}_3)_2]$ (**1**) showing 30% thermal ellipsoids.

Table 1. Crystallographic Data for $[\text{RuCl}(\text{nMePPh})(\text{PPh}_3)_2]$ (1**) and $[\text{RuCl}(\text{nMePPh})(\text{EtOH})(\text{PPh}_3)\cdot 0.64(\text{Me})_2\text{CO}]$ (**2**)**

	1	2
chemical formula	$\text{C}_{51}\text{H}_{53}\text{B}_9\text{ClP}_3\text{Ru}$	$\text{C}_{35}\text{H}_{44}\text{B}_9\text{OClP}_2\text{Ru}\cdot 0.64(\text{Me})_2\text{CO}$
fw	992.71	813.66
<i>a</i> (Å)	10.626(2)	16.878 (4)
<i>b</i> (Å)	19.270(3)	19.377 (5)
<i>c</i> (Å)	24.105(2)	13.811 (3)
α (deg)	90.0	103.15 (2)
β (deg)	97.74(1)	97.14 (2)
γ (deg)	90.0	79.31 (2)
<i>V</i> (Å ³)	4891(1)	4306 (4)
<i>Z</i>	4	4
space group	monoclinic $P2_1/n$ (No. 14)	triclinic $P\bar{1}$ (No. 2)
<i>T</i> (°C)	23	
λ (Å)	0.71069	0.71069
ρ (g cm ⁻³)	1.348	1.255
μ (cm ⁻¹)	5.00	5.2
transm coeff	0.910–1.000	0.936–1.000
<i>R</i> (<i>F</i> _o)	0.041	0.071
<i>R</i> _w (<i>F</i> _o)	0.056	0.077

structures, crystals of **1** and **2** were grown and their structures determined. The crystallographic data are indicated in Table 1. No crystals of the hydride series have been obtained yet, but work is in progress.

The structure of $[\text{RuCl}(\text{nMePPh})(\text{PPh}_3)_2]$ (**1**) confirms that isomer C in Figure 4 has been formed. In the complex unit the Ru(II) atom is bonded octahedrally to the tridentate *nido*-carborane cage, the chloride ion, and two phosphorus atoms of two triphenylphosphine groups (cf. Figure 11). The three bonds from the cage to Ru(II) are formed by the phosphorus atom of the diphenylphosphine group and two hydrogen atoms bonded to B(2) and B(11). In the coordination sphere, the cluster P atom and the P atom of one triphenylphosphine are in *trans* positions to each other, and BH(2) is *trans* to the P atom of the second PPh₃ ligand. The BH(11) is *trans* to the Cl. Selected bonding parameters are given in Table 2.

The coordination sphere around the Ru(II) ion in **1** is very crowded. The Ru–P bond lengths are 2.465(2), 2.395(2), and 2.305(2) Å for the Ru(1)–P(1), Ru(1)–P(2), and Ru(1)–P(3) bonds, respectively. These bond lengths are comparable to those found in *trans*- $[\text{Ru}(\text{nMePPh})_2]\cdot 2\text{Me}_2\text{CO}$ and *cis*- $[\text{Ru}(\text{nMePPh})_2]\cdot 1.486\text{CHCl}_3$.¹ The two longer Ru–P bonds are due to the *trans* influence. The observed Ru(1)–B(2) and Ru(1)–B(11) distances are 2.473(2) and 2.422(8) Å, respectively, with Ru(1)–H(2) and Ru(1)–H(11) bond lengths of 2.00(6) and 1.78(5) Å.

In the complex unit of **1** the *trans*-P–Ru–P angle is 164.63(6)° and the *cis*-P–Ru–P angle is opened to 95.43(6)°, compared to the ideal angle (90°) of an octahedral coordination sphere. Other values for octahedral angles

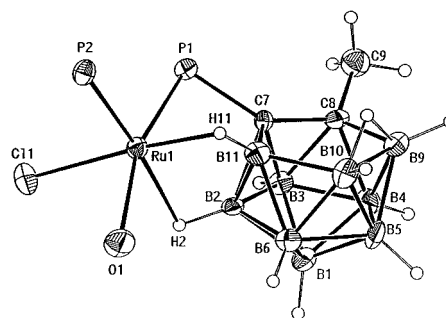


Figure 12. Simplified ORTEP view of molecule I of $[\text{RuCl}(\text{nMePPh})(\text{EtOH})(\text{PPh}_3)]\cdot 0.64(\text{Me})_2\text{CO}$ (**2**) showing 30% thermal ellipsoids.

Table 2. Selected Interatomic Distances (Å) and Angles (deg) (Esd's in Parentheses) for $[\text{RuCl}(\text{nMePPh})(\text{PPh}_3)_2]$ (1**)**

Ru(1)–Cl(1)	2.411(2)	P(2)–C(41)	1.850(7)
Ru(1)–P(1)	2.465(2)	P(2)–C(51)	1.861(7)
Ru(1)–P(2)	2.395(2)	P(3)–C(61)	1.848(7)
Ru(1)–P(3)	2.305(2)	P(3)–C(71)	1.831(6)
Ru(1)–B(2)	2.473(8)	P(3)–C(81)	1.838(6)
Ru(1)–B(11)	2.422(8)	C(7)–C(8)	1.561(8)
Ru(1)–H(2)	2.00(6)	C(7)–B(2)	1.730(9)
Ru(1)–H(11)	1.78(5)	C(7)–B(11)	1.613(9)
P(1)–C(7)	1.815(6)	C(8)–B(9)	1.65(1)
P(1)–C(11)	1.834(6)	B(9)–B(10)	1.89(1)
P(1)–C(21)	1.826(6)	B(10)–B(11)	1.77(1)
P(2)–C(31)	1.847(6)		
Cl(1)–Ru(1)–P(1)	100.05(6)	P(3)–Ru(1)–H(2)	172(2)
Cl(1)–Ru(1)–P(2)	88.88(6)	P(3)–Ru(1)–H(11)	99(2)
Cl(1)–Ru(1)–P(3)	93.37(6)	H(2)–Ru(1)–H(11)	87(2)
Cl(1)–Ru(1)–H(2)	80(2)	Ru(1)–P(1)–C(7)	84.6(2)
Cl(1)–Ru(1)–H(11)	167(2)	Ru(1)–P(1)–C(11)	125.2(2)
P(1)–Ru(1)–P(2)	164.63(6)	Ru(1)–P(1)–C(21)	124.4(2)
P(1)–Ru(1)–P(3)	95.43(6)	P(1)–C(7)–C(8)	132.4(4)
P(1)–Ru(1)–H(2)	81(2)	P(1)–C(7)–B(2)	106.9(4)
P(1)–Ru(1)–H(11)	73(2)	P(1)–C(7)–B(11)	103.6(4)
P(2)–Ru(1)–P(3)	96.52(6)	C(8)–C(7)–B(2)	113.2(5)
P(2)–Ru(1)–H(2)	89(2)	C(8)–C(7)–B(11)	117.5(5)
P(2)–Ru(1)–H(11)	95(2)		

also deviate from the ideal ones. The distortions can be due to steric crowding of the bulky PPh₂ groups and due to the rigid tridentate carborane ligand, which is not able to bond ideally.

$[\text{RuCl}(\text{nMePPh})(\text{EtOH})(\text{PPh}_3)]\cdot 0.64(\text{Me})_2\text{CO}$ (**2**) has a structure very similar to that of **1**. In this case, the ethanol molecule has replaced one phosphine molecule and is *trans* to the *exo*-cluster P atom. The asymmetric unit of **2** contains two $[\text{RuCl}(\text{nMePPh})(\text{EtOH})(\text{PPh}_3)]$ complex units (one is shown in Figure 12) and disordered acetone molecules from crystallization. These occupy empty places in the lattice. The octahedral complex units are approximately mirror images of each other. The corresponding bond lengths and angles of both molecules (Table 3) in the asymmetric unit are quite similar, but not identical. The most striking difference between the two molecules is the different position of the coordinated ethanol molecules. In molecule I, the ethanol molecule is disordered with the ethyl group assuming two orientations, while in molecule II, the ethanol is located in one position. In molecule I of **2** the P–Ru–O angle is 162.8(2)° and the *cis*-P–Ru–P angle is 98.6(1)°. Those angles in molecule II are 163.5(2)° and 98.1(1)°. Thus, the *cis*-P–Ru–P angle is increased ca. 3° in the displacement compound **2** vs **1**.

It was mentioned before that the coordination sphere of Ru(II) ion is very crowded in **1**. The replacement of one triphenylphosphine group by ethanol seems to

Table 3. Selected Interatomic Distances (Å) and Angles (deg) (Esd's in Parentheses) for [RuCl(nMePPh)(EtOH)(PPh₃)]·0.64(Me)₂CO (2**)**

Molecule I			
Ru(1)–Cl(1)	2.410(3)	Ru(1)–P(1)	2.276(4)
Ru(1)–P(2)	2.270(3)	Ru(1)–O(1)	2.224(9)
Ru(1)–B(2)	2.44(1)	Ru(1)–B(11)	2.34(1)
Ru(1)–H(2)	2.06	Ru(1)–H(11)	1.83
P(1)–C(7)	1.808(9)	P(1)–C(31)	1.820(9)
P(1)–C(37)	1.81(1)	P(2)–C(43)	1.842(7)
P(2)–C(49)	1.824(6)	P(2)–C(55)	1.82(1)
C(7)–C(8)	1.54(1)	C(7)–B(11)	1.62(2)
C(8)–C(9)	1.53(2)	C(8)–B(9)	1.64(2)
B(9)–B(10)	1.89(2)	B(10)–B(11)	1.79(2)
Cl(1)–Ru(1)–P(1)	104.3(1)	P(1)–C(7)–C(8)	137.1(8)
Cl(1)–Ru(1)–P(2)	93.1(1)	P(1)–C(7)–B(2)	103.2(6)
Cl(1)–Ru(1)–H(11)	174	P(1)–C(7)–B(3)	120.2(6)
P(1)–Ru(1)–P(2)	98.6(1)	P(1)–C(7)–B(11)	101.0(7)
P(1)–Ru(1)–O(1)	162.8(2)	C(8)–C(7)–B(11)	117.1(8)
P(2)–Ru(1)–H(2)	175	C(7)–C(8)–B(9)	109.0(9)
H(2)–Ru(1)–H(11)	92	C(8)–B(9)–B(10)	107.2(9)
Ru(1)–P(1)–C(7)	87.5(4)	B(9)–B(10)–B(11)	100.1(9)
Ru(1)–P(1)–C(31)	125.7(4)	C(7)–B(11)–B(10)	106(1)
Ru(1)–P(1)–C(37)	120.9(5)		
Molecule II			
Ru(2)–Cl(2)	2.400(3)	P(3)–C(67)	1.819(8)
Ru(2)–P(3)	2.277(4)	P(4)–C(73)	1.838(6)
Ru(2)–P(4)	2.267(3)	P(4)–C(79)	1.83(2)
Ru(2)–O(2)	2.189(9)	P(4)–C(85)	1.84(1)
Ru(2)–B(22)	2.49(1)	C(27)–C(28)	1.54(2)
Ru(2)–B(31)	2.38(1)	C(27)–B(31)	1.60(2)
Ru(2)–H(22)	2.11	C(28)–C(29)	1.49(2)
Ru(2)–H(31)	1.85	C(28)–B(29)	1.63(2)
P(3)–C(27)	1.814(9)	B(29)–B(30)	1.91(2)
P(3)–C(61)	1.824(7)	B(30)–B(31)	1.75(2)
Cl(2)–Ru(2)–P(3)	104.7(1)	P(3)–C(27)–C(28)	135.6(8)
Cl(2)–Ru(2)–P(4)	92.6(1)	P(3)–C(27)–B(22)	104.4(7)
Cl(2)–Ru(2)–H(31)	175	P(3)–C(27)–B(23)	120.8(6)
P(3)–Ru(2)–P(4)	98.1(1)	P(3)–C(27)–B(31)	101.4(6)
P(3)–Ru(2)–O(2)	163.5(2)	C(28)–C(27)–B(31)	116.6(8)
P(4)–Ru(2)–H(22)	177	C(27)–C(28)–B(29)	108.6(9)
H(22)–Ru(2)–H(31)	91	C(28)–B(29)–B(30)	107.5(9)
Ru(2)–P(3)–C(27)	87.6(4)	C(27)–B(31)–B(30)	108.5(9)
Ru(2)–P(3)–C(61)	124.6(3)	B(29)–B(30)–B(31)	98.6(9)
Ru(2)–P(3)–C(67)	122.7(3)		

release that. The Ru–P bond lengths in **2** range from 2.267(3) to 2.277(2) Å and those in **1** range from 2.465(2) to 2.305(2) Å. The Ru(1)–B(11) distance of 2.473(2) Å in **1** has decreased to 2.34(1) Å in molecule I of **2**. Thus, it seems that the boron cage can get closer to Ru(II) if one PPh₃ ligand of **1** is replaced by an ethanol molecule.

The coordination of the [nMePPh₂][−] ligand to the Ru(II) ion modifies the ligand. This could be found by comparing the typical values of the angles in the free and coordinated ligands. As we do not have the crystal structure of this ligand, we can use a very close derivative as an example. In [NMe₄][7,8-(PPh₂)₂-7,8-C₂B₉H₁₀],¹¹ the P–C(7)–C(8) angles are ca. 115° and the P–C(7)–B(2) and P–C(7)–B(11) angles are ca. 125°. In the chemical **1**, the values for angles P(1)–C(7)–C(8), P(1)–C(7)–B(2), and P(1)–C(7)–B(11) are 132.4(4)°, 106.9(4)°, and 103.6(4)°, respectively. These values show that in **1** the phosphorus atom is moved away from C(8) toward B(2) and B(11), thus opening the P(1)–C(7)–C(8) angle from 115° to 132.4(4)°. In complex **2**, the P(1)–C(7)–C(8) angle is opened to 137.1(8)° for I and 135.6(8)° for II. Consequently, the P(1)–C(7)–B(2) and P(1)–C(7)–B(11) angles are diminished to 103.2-

(6)° and 101.0(7)°, respectively, and in unit II the equivalent values are 104.4(7)° and 101.4(6)°, respectively. It seems obvious that the tricoordination of the *nido* studied cage modifies the bond between the boron cage and the phosphorus atom bonded to it. Similar movement of the phosphorus atom has been reported for the two isomers of [Ru(nMePPh)₂].¹

Modulation of the B(11)–H→Ru and B(2)–H→Ru Resonances. The ¹H NMR spectra of the compounds described in the different series contribute considerably to the understanding of the factors influencing the B(11)–H→Ru and B(2)–H→Ru resonances in these [C₂B₉H₁₂][−] derivatives. First, it is clear that C(8)–R substitution on the cluster has little effect on the B(11)–H→Ru and B(2)–H→Ru resonances. This can be seen in Table 4 by looking at the entries [RuCl(nHPPPh)(PPh₃)₂], [RuCl(nPhPPh)(PPh₃)₂], and [RuCl(nMePPh)(PPh₃)₂], all having constant ancillary ligands and differing only in the substituent on C(8). The B(11)–H→Ru resonances range from −14.80 to −14.90 ppm and the B(2)–H→Ru resonances from −3.42 to −3.71 ppm. Thus, we feel that the introduction of large groups on C(8) would induce little effect on the B(11)–H→Ru and B(2)–H→Ru bonds. The substitution of the R' groups on the *exo*-cluster PR'₂ does not affect these resonances either, though some modulation has been produced. In [RuCl(nMePEt)(PPh₃)₂] (**10**) the result of substituting *exo*-cluster PPh₂ by the more basic *exo*-cluster PEt₂ group is a shift in the B(2)–H→Ru resonance to −4.05 ppm and the B(11)–H→Ru to −15.20 ppm. So it seems that B(2)–H→Ru is more influenced than B(11)–H→Ru by this substitution.

On the other hand, *cis* influence seems to be of little relevance too, as it is observed in compounds **2** and **3**. These compounds have the structure indicated in Figure 5. The EtOH or tht is *cis* to the B–H's and the B–H→Ru resonances do not differ greatly from the values found for **1**, though some variation in the chemical shift has been experienced by B(2)–H→Ru.

The major shift has been produced by the ligands *trans* to the B–H→Ru studied. Let us first consider the compounds *trans*-[Ru(nMePPh)₂] and *cis*-[Ru(nMePPh)₂]. A BH *trans* to a B–H→Ru produces resonances at −11.20 [B(11)–H→Ru] and −10.32 ppm [B(2)–H→Ru]. These assignments are tentative. Substitution of a *trans*-BH by an *exo*-cluster PPh₂ in *cis*-[Ru(nMePPh)₂] shifts the B(2)–H→Ru signal to −5.55 ppm. To quantify this *trans* influence, *I*(*y*), the following equation is proposed:

$$[B(x)–H→Ru](y) - [B(x)–H→Ru](BH) = I(y) \quad (3)$$

where [B(*x*)–H→Ru](*y*) indicates the resonance corresponding to the boron *x trans* influenced by *y* and [B(*x*)–H→Ru](BH) corresponds to the same boron *trans* influenced by BH.

In *cis*-[Ru(nMePPh)₂] the *I*(PR₃) value would be +4.7. In the series [RuCl(nRPPPh)(PPh₃)₂] (R = Me, H, Ph) the *I*(PR₃) would be slightly greater, between +6.9 and +6.6. Getting the precise figures would require one to consider many examples and quantify the effects of *cis* influence and the nature of the R radicals in PR₃ ligands. Though of only qualitative value, these *I*(*y*) values will be helpful in making predictions. Where several data are available we have applied the average value. For *I*(PR₃) we propose a value of +6 ppm. By following eq 3, we have found for *I*(CO) a value of +4.3 ppm. The *I*(H) can be

(11) Teixidor, F.; Viñas, C.; Abad, M. M.; Nuñez, R.; Kivekäs, R.; Sillanpää, R. *J. Organomet. Chem* **1995**, *503*, 193.

Table 4. ^1H NMR Chemical Shifts for (B–H–B) and B(x)–H–Ru Resonances

compounds	B–H–B	B(2)–H–Ru	B(11)–H–Ru	Ru–H
<i>trans</i> -[Ru(nMePPh) ₂]	-2.73	-10.32	-11.20	
<i>cis</i> -[Ru(nMePPh) ₂]	-2.87	-5.55	-10.70	
[RuCl(nMePPh)(PPh ₃) ₂] (1)	-3.39	-3.42	-14.90	
[RuCl(nMePPh)(EtOH)(PPh ₃) ₂] (2)	-3.14	-1.06	-15.01	
[RuCl(nMePPh)(tth)(PPh ₃) ₂] (3)	-3.50	-2.40	-15.20	
[RuCl(nMePPh)(CO)(PPh ₃) ₂] (4)	-3.25	-6.05	-15.01	
[RuCl(nHPPh)(PPh ₃) ₂] (5)	-3.61	-3.50	-14.90	
[RuCl(nPhPPh)(PPh ₃) ₂] (6)	-2.90	-3.71	-14.80	
[RuH(nMePPh)(PPh ₃) ₂] (7)	-2.86	-6.41	-2.03	-13.46
[RuH(nHPPh)(PPh ₃) ₂] (8)	-3.10	-6.95	-2.10	-13.80
[RuH(nPhPPh)(PPh ₃) ₂] (9)	-2.40	-6.75	-1.80	-13.90
[RuCl(nMePEt)(PPh ₃) ₂] (10)	-3.11	-4.05	-15.20	
[NMe ₄][nMePPh]	-2.24			
[NMe ₄][nHPPh]	-2.24			
[NBu ₄][nPhPPh]	-2.29			
[NBu ₄][nMePEt]	-2.55			

Table 5. $^1J(\text{B,H})$ for B(11)–H–Ru Resonances from ^1H and ^{11}B NMR Spectra for the Complexes 1 and 7, 5 and 8, and 6 and 9

R	$^1J(\text{B,H})$, series H ⁻ (Hz)	$^1J(\text{B,H})$, series Cl ⁻ (Hz)
H	106	86
Ph	106	86
Me	108	83

studied by looking at the series [RuH(nRPPh)(PPh₃)₂] and focusing on B(11)–H–Ru. The $I(\text{H})$ is the largest that we have found. The average value for the three compounds 7–9 is $I(\text{H}) = +8.5$ ppm. The $I(\text{H})$ is so high that it even alters the $I(\text{PR}_3)$ in these compounds, e.g., the PR₃ *trans* influence on its BH is weakened and the chemical shifts obtained are more negative than would be expected according to the $I(\text{PR}_3) = +6$ ppm given earlier. This is why the values of the H⁻ series have not been included in calculating $I(\text{PR}_3)$. The $I(\text{Cl})$ may be calculated in a similar way to give a negative value; in this case $I(\text{Cl}) = -3.8$ ppm. These values agree with the sequence $I(\text{H}) > I(\text{PR}_3) > I(\text{CO}) > I(\text{BH}) > I(\text{Cl})$.

This sequence resembles the known *trans* influence,¹² which should permit a predefined modulation of the B(2)–H–Ru and B(11)–H–Ru resonances.

The B(11)–H–Ru resonances found in the chloride series are very comparable to the M–H values in the hydride series, which proves our initial assumption about two extreme types of agostic bonds, which are shown in Figure 2. The $^1J(\text{B,H})$ data also confirm this assumption.¹³ As indicated in the former sequence, the two extreme cases are those for $I(\text{H})$ and $I(\text{Cl})$. By focusing on these series, we have observed that $^1J(\text{B,H})$ of the boron atom *trans* to Y differs depending on the nature of Y, e.g., $^1J(\text{B,H}) \approx 106$ Hz for Y = H⁻ or $^1J(\text{B,H}) \approx 83$ Hz for Y = Cl⁻. This means that for Y = Cl⁻ the B–H bond is weaker than that for Y = H⁻, or in another way, for Y = Cl⁻ there is more M–H character than for Y = H⁻ (see Table 5).

Conclusions

It has been possible to activate the B(2)–H and B(11)–H groups of the [C₂B₉H₁₂]⁻ *nido* cage by coordination to Ru(II) in a cooperative way with an *exo*-cluster PR₂ group. The ^1H NMR resonances of the B(2)–H–Ru and B(11)–H–Ru hydrogens may be modulated by modifying the nature of the ruthenium ancillary ligands.

(12) Cotton, F. A.; Wilkinson, G. *Advanced Inorganic Chemistry*, 5th ed.; Wiley Interscience: New York, 1984; p 1300.

(13) We thank one of the referees for this suggestion.

In that case both B(2)–H–Ru and B(11)–H–Ru bonds can be modulated. A *trans* influence seems to be the reason for this modulation. A tentative order of the *trans* influence would be $I(\text{H}) > I(\text{PR}_3) > I(\text{CO}) > I(\text{BH}) > I(\text{Cl})$.

Experimental Section

Instrumentation. Elemental analyses were performed in our analytical laboratory using a Carlo Erba EA1108 microanalyzer. IR spectra were obtained with KBr pellets on a Nicolet 710-FT spectrophotometer. The ^1H NMR, ^{11}B NMR, and ^{31}P NMR spectra were obtained by using Bruker AM 400WB and Bruker ARX 300 instruments.

Materials. Before use, methyl-*o*-carborane, *o*-carborane, and decaborane (Dexsil Chemical Corp.) were sublimed under high vacuum; [NMe₄][nMePPh], [NMe₄][nHPPh], and [NBu₄][nMePEt] were prepared according to the literature.¹¹ 1-PPh₂-2-Ph-1,2-C₂B₁₀H₁₀¹⁴ was prepared from phenyl-*o*-carborane,¹⁵ which was prepared from decaborane. [RuCl₂(PPh₃)₃] and [Ru(AcO)H(PPh₃)] were synthesized according to the literature,¹⁶ and RuCl₃·xH₂O from Johnson Matthey was used as purchased. Ethanol was reagent grade. All reactions were carried out under a dinitrogen atmosphere. All solvents were deoxygenated before use.

Synthesis of [NBu₄][nPhPPh]. To 40 mL of deoxygenated toluene containing 400 mg (0.990 mmol) of 1-PPh₂-2-Ph-1,2-C₂B₁₀H₁₀ was added piperidine (4.20 g, 49.50 mmol). The solution was stirred and refluxed for 26 h. Once cooled, the solvent was evaporated and the residue was dissolved in ethanol (15 mL). A solution of tetrabutylammonium bromide in water (15 mL) was added while dinitrogen was bubbled into the ethanolic solution. A white solid precipitated. This was filtered off and washed with water (10 mL) and ethyl ether (10 mL) to yield 0.55 g (87%). FTIR (KBr): ν_{max} (B–H) = 2523 cm⁻¹. ^1H FTNMR (300 MHz, (CD₃)₂CO, 25 °C, TMS): δ -2.29 (br, 1 H, BHB), 0.99 (t, $^1J(\text{H,H}) = 7.2$ Hz, 12 H, CH₃), 1.36 (hex, $^1J(\text{H,H}) = 7.2$ Hz, 8 H, CH₂), 1.60 (m, 8 H, CH₂), 3.09 (t, $^1J(\text{H,H}) = 8.2$ Hz, 8 H, CH₂), 6.66–7.85 (m, 15 H, C_{aryl}-H). ^{11}B FTNMR (96 MHz, (CD₃)₂CO, 25 °C, BF₃·Et₂O): δ -6.6 (d, $^1J(\text{B,H}) = 172$ Hz, 1 B), -9.8 (d, $^1J(\text{B,H}) = 134$ Hz, 1 B), -15.9 (4 B), -22.2 (1 B), -32.2 (1 B), -34.5 (d, $^1J(\text{B,H}) = 134$ Hz, 1 B). $^{31}\text{P}\{^1\text{H}\}$ FTNMR (121 MHz, (CD₃)₂CO, 25 °C, H₃PO₄): δ = 39.96 (s). Anal. Calcd for C₃₈H₆₁B₉NP: C, 67.9; H, 9.66; N, 2.20. Found: C, 67.43; H, 9.55; N, 2.19.

Synthesis of [RuCl(nMePPh)(PPh₃)₂] (1). (A) To 50 mL of ethanol solution containing 100 mg (0.247 mmol), of [NMe₄]

(14) Zakharkin, L. I.; Zhubekova, M. N.; Kazantsev, A. V. *Zh. Obshch. Khim.* **1972**, 5, 42.

(15) Fein, M. M.; Grafstein, D.; Paustian, J. E.; Bobinski, J.; Lichstein, B. M.; Mayes, N.; Schwartz, N. N.; Cohen, M. S. *Inorg. Chem.* **1963**, 2, 1115.

(16) (a) Hallman, P. S.; Stephenson, T. A.; Wilkinson, G. *Inorg. Synth.* **1970**, 12, 237. (b) Mitchel, R. W.; Spencer, A.; Wilkinson, G. *J. Chem. Soc., Dalton Trans.* **1973**, 846.

[nMePPh] was added [RuCl₂(PPh₃)₃] (237 mg, 0.247 mmol), and the mixture was refluxed for 2 h. A dark orange solid precipitated. The solution was allowed to cool and the solid was filtered off, washed with three portions (5 mL) of ethanol, and air dried. Yield: 170 mg (70%). FTIR (KBr): ν_{\max} (B–H) = 2551, 2530 cm⁻¹. ¹H{¹H} FTNMR (400 MHz, CDCl₃, 25 °C, TMS): δ -14.90 (br, 1 H, BHRu), -3.42 (d, ²J(H,P) = 38 Hz, 1 H, BHRu), -3.39 (s, 1 H, BHB), 1.03 (s, 3 H, CH₃), 6.74–8.24 (m, 40 H, C_{aryl}-H). ¹H FTNMR (400 MHz, CDCl₃, 25 °C, TMS): δ -14.90 (br, 1 H, BHRu), -3.42 (br, 1 H, BHRu), -3.39 (br, 1 H, BHB), 1.03 (s, 3 H, CH₃), 6.74–8.24 (m, 40 H, C_{aryl}-H). ¹¹B FTNMR (128 MHz, CDCl₃, 25 °C, BF₃·Et₂O): δ 3.37 (1 B), -12.87 (1 B), -16.31 (2 B), -18.47 (d, ¹J(B,H) = 83 Hz, 1 B), -20.47 (d, ¹J(B,H) = 134 Hz, 1 B), -31.01 (2 B), -38.94 (1 B). ³¹P{¹H} FTNMR (161 MHz, CDCl₃, 25 °C, H₃PO₄, 85%): δ 14.34 (dd, ²J(P,P)_c = 37 Hz, ²J(P,P)_t = 294 Hz), 27.34 (dd, 1 P, ²J(P,P)_c = 24 Hz, ²J(P,P)_t = 294 Hz), 46.17 (dd, 1 P, ²J(P,P)_c = 37 Hz, ²J(P,P)_c = 24 Hz). Anal. Calcd for C₅₁H₅₃B₉P₃ClRu: C, 61.71; H, 5.38. Found: C, 61.62; H, 5.51.

(B) RuCl₃·nH₂O (30 mg, 0.125 mmol) was added to methanol (10 mL), and the solution was refluxed for 5 min. After cooling, 65 mg (0.247 mmol) of PPh₃ and 100 mg (0.247 mmol) of [NMe₄][nMePPh] were added. The mixture was refluxed for 2 h and an orange solid precipitated. The solution was cooled at room temperature, and the solid was filtered off and washed with methanol (10 mL) and ethyl ether (10 mL). Yield: 45 mg (18%). The analyses and characterization of [RuCl(nMePPh)](PPh₃)₂ were the same as before. Orange crystals suitable for X-ray analysis were grown from dichloromethane/acetone (1:1) solution after slow evaporation.

Preparation of [RuCl(nMePPh)(EtOH)(PPh₃)] (2). To a solution of non-deoxygenated chloroform/ethanol/acetone (0.5:0.5:1) was added **1**. After 15 days, red crystals suitable for X-ray analysis were grown from this solution by slow evaporation. FTIR (KBr): ν_{\max} (B–H) = 2551, 2530 cm⁻¹. ¹H FTNMR (400 MHz, CDCl₃, 25 °C, TMS): δ -15.01 (br, 1 H, BHRu), -3.14 (br, 1 H, BHB), -1.06 (br, 1 H, BHRu), 1.19 (s, 3 H, CH₃), 6.74–8.14 (m, 25 H, C_{aryl}-H). ¹¹B FTNMR (128 MHz, CDCl₃, 25 °C, BF₃·Et₂O): δ 2.95 (1 B), -10.39 (1 B), -13.69 (2 B), -15.85 (d, ¹J(B,H) = 84 Hz, 1 B), -18.62 (d, ¹J(B,H) = 122 Hz, 1 B), -27.39 (2 B), -36.04 (d, ¹J(B,H) = 136 Hz, 1 B). ³¹P{¹H} FTNMR (161 MHz, CDCl₃, 25 °C, H₃PO₄, 85%): δ 36.40 (d, ²J(P,P)_c = 42 Hz, 1 P), 68.08 (d, ²J(P,P)_c = 42 Hz, 1 P). Anal. Calcd for C₃₅H₄₄B₉OP₂ClRu·0.64-(Me)₂CO: C, 54.49; H, 5.88. Found: C, 54.50; H, 5.90.

Preparation of [RuCl(nMePPh)(tth)(PPh₃)] (3). To 2 mL of non-deoxygenated chloroform solution containing 50 mg (0.050 mmol) of **1** was added tetrahydrothiophene (5 mg, 0.06 mmol), and the mixture was stirred for 10 days at room temperature. The solvent was removed and the residue was treated with dichloromethane and acetone, giving a red solid. Yield: 15 mg (35%). FTIR (KBr): ν_{\max} (B–H) = 2572, 2544 cm⁻¹. ¹H FTNMR (300 MHz, CDCl₃, 25 °C, TMS): δ -15.20 (br, 1 H, BHRu), -3.50 (br, 1 H, BHB), -2.40 (br, 1 H, BHRu), 1.29 (s, 3 H, CH₃), 1.88 (m, 4 H, CH₂), 2.61 (m, 4 H, CH₂), 6.57–8.08 (m, 25 H, C_{aryl}-H). ¹¹B{¹H} FTNMR (96 MHz, CDCl₃, 25 °C, BF₃·Et₂O): δ -6.20 (1 B), -4.50 (1 B), -15.63 (2 B), -17.90 (1 B), -19.70 (1 B), -29.20 (2 B), -36.40 (1 B). ³¹P{¹H} FTNMR (121 MHz, CDCl₃, 25 °C, H₃PO₄, 85%): δ 15.03 (dd, ²J(P,P)_c = 39 Hz, 1 P), 61.63 (d, ²J(P,P)_c = 39 Hz, 1 P). Anal. Calcd for C₃₇H₄₆B₉P₂SClRu: C, 54.31; H, 5.63; S, 3.91. Found: C, 55.01; H, 5.70; S, 3.65.

Preparation of [RuCl(nMePPh)(CO)(PPh₃)] (4). A stream of CO was passed through a solution of 40 mg (0.040 mmol) of **1** in chloroform (10 mL) by stirring. The solution, which became pale yellow, was treated with ethyl ether (10 mL) and hexane (10 mL) and a yellow solid precipitated. The solid was filtered off, washed with hexane (10 mL), and dried. Yield: 15 mg (50%). FTIR (KBr): ν_{\max} (B–H) = 2551, 2530 cm⁻¹, ν_{\max} (C=O) = 2031 cm⁻¹. ¹H FTNMR (300 MHz, CDCl₃, 25 °C, TMS): δ -15.01 (br, 1 H, BHRu), -3.25 (br, 1 H, BHB), -6.05 (br, 1 H, BHRu), 1.27 (s, 3 H, CH₃), 7.27–7.94 (m, 25 H, C_{aryl}-H). ¹¹B{¹H} FTNMR (96 MHz, CDCl₃, 25 °C, BF₃·

Et₂O): δ -0.59 (1 B), -12.27 (3 B), -21.79 (2 B), -24.07 (1 B), -26.89 (1 B), -33.80 (1 B). ³¹P{¹H} FTNMR (121 MHz, CDCl₃, 25 °C, H₃PO₄, 85%): δ -7.48 (d, ²J(P,P)_t = 236 Hz, 1 P), 24.28 (d, ²J(P,P)_t = 236 Hz, 1 P). Anal. Calcd for C₃₃H₃₈B₉OP₂ClRu: C, 53.11; H, 5.09. Found: C, 54.05; H, 5.15.

Synthesis of [RuCl(nHPPh)(PPh₃)₂] (5). To 20 mL of ethanol solution containing 75 mg (0.191 mmol) of [NMe₄]-[nHPPh] was added [RuCl₂(PPh₃)₃] (183 mg, 0.191 mmol), and the mixture was refluxed for 2 h. A dark orange solid precipitated. The solution was allowed to cool, and the orange solid was filtered off, washed with three portions (5 mL) of ethanol, and dried. Yield: 156 mg (83%). FTIR (KBr): ν_{\max} (B–H) = 2614, 2572, 2523 cm⁻¹. ¹H{¹H} FTNMR (250 MHz, CDCl₃, 25 °C, TMS): δ -14.90 (br, 1 H, BHRu), -3.61 (s, 1 H, BHB), -3.50 (d, ²J(H,P) = 38 Hz, 1 H, BHRu), 2.04 (s, 1 H, CH), 6.42–8.12 (m, 40 H, C_{aryl}-H). ¹H FTNMR (250 MHz, CDCl₃, 25 °C, TMS): δ -14.90 (br, 1 H, BHRu), -3.61 (br, 1 H, BHB), -3.50 (br, 1 H, BHRu), 2.04 (s, 1 H, CH), 6.42–8.12 (m, 40 H, C_{aryl}-H). ¹¹B FTNMR (96 MHz, CD₂Cl₂, 25 °C, BF₃·Et₂O): δ 5.67 (1 B), -16.50 (2 B), -17.57 (d, ¹J(B,H) = 86 Hz, 1 B), -19.19 (2 B), -27.38 (1 B), -30.32 (1 B), -36.67 (1 B). ³¹P{¹H} FTNMR (121 MHz, CD₂Cl₂, 25 °C, H₃PO₄, 85%): δ 4.50 (dd, ²J(P,P)_c = 38 Hz, ²J(P,P)_t = 297 Hz, 1 P), 26.25 (dd, ²J(P,P)_c = 25 Hz, ²J(P,P)_t = 297 Hz, 1 P), 47.62 (dd, ²J(P,P)_c = 38 Hz, ²J(P,P)_c = 25 Hz, 1 P). Anal. Calcd for C₅₀H₅₁B₉P₃ClRu: C, 61.36; H, 5.25. Found: C, 60.66; H, 5.05.

Synthesis of [RuCl(nPhPPh)(PPh₃)₂] (6). To 25 mL of ethanol solution containing 100 mg (0.157 mmol) of [NBu₄]-[nPhPPh] was added [RuCl₂(PPh₃)₃] (150 mg, 0.157 mmol), and the mixture was refluxed for 3.5 h. A dark orange solid precipitated. The solid was filtered off while warm, washed with three portions (5 mL) of ethanol, and dried. Yield: 123 mg (74%). FTIR (KBr): ν_{\max} (B–H) = 2572, 2530 cm⁻¹. ¹H FTNMR (300 MHz, CDCl₃, 25 °C, TMS): δ -14.80 (br, 1 H, BHRu), -3.71 (br, 1 H, BHRu), -2.90 (br, 1 H, BHB), 6.62–8.10 (m, 45 H, C_{aryl}-H). ¹¹B{¹H} FTNMR (96 MHz, CDCl₃, 25 °C, BF₃·Et₂O): δ 7.15 (1 B), -14.28 (3 B), -17.40 (2 B), -29.20 (2 B), -37.00 (1 B). ³¹P{¹H} FTNMR (121 MHz, CDCl₃, 25 °C, H₃PO₄, 85%): δ 15.20 (dd, ²J(P,P)_c = 36 Hz, ²J(P,P)_t = 293 Hz, 1 P), 24.62 (dd, ²J(P,P)_c = 25 Hz, ²J(P,P)_t = 293 Hz, 1 P), 44.93 (dd, ²J(P,P)_c = 36 Hz, ²J(P,P)_c = 25 Hz, 1 P). Anal. Calcd for C₅₆H₅₅B₉P₃ClRu: C, 63.77; H, 5.26. Found: C, 63.61; H, 4.82.

Synthesis of [RuH(nMePPh)(PPh₃)₂] (7). To 15 mL of ethanol solution containing 35 mg (0.086 mmol) of [NMe₄]-[nMePPh] was added [Ru(AcO)H(PPh₃)₃] (82 mg, 0.086 mmol), and the mixture was refluxed for 30 min. A light yellow solid precipitated. The solid was filtered off, washed with three portions (5 mL) of ethanol, and dried. Yield: 31 mg (37%). FTIR (KBr): ν_{\max} (B–H) = 2551, 2530, 2502 cm⁻¹, ν_{\max} (Ru–H) = 1996 cm⁻¹. ¹H FTNMR (400 MHz, (CD₃)₂CO, 25 °C, TMS): δ -13.46 (br, 1 H, RuH), -6.41 (br, 1 H, BHRu), -2.86 (br, 1 H, BHB), -2.03 (tetrap, ¹J(H,B) = 108 Hz, 1 H, BHRu), 1.13 (s, 3 H, CH₃), 6.52–8.25 (m, 40 H, C_{aryl}-H). ¹¹B FTNMR (128 MHz, (CD₃)₂CO, 25 °C, BF₃·Et₂O): δ 2.38 (1 B), -13.49 (3 B), -17.38 (d, ¹J(B,H) = 108 Hz, 1 B), -20.34 (d, ¹J(B,H) = 132 Hz, 1 B), -29.73 (2 B), -36.62 (d, ¹J(B,H) = 142 Hz, 1 B). ³¹P{¹H} FTNMR (101 MHz, (CD₃)₂CO, 25 °C, H₃PO₄, 85%): δ 39.49 (dd, ²J(P,P)_c = 39 Hz, ²J(P,P)_t = 250 Hz, 1 P), 53.98 (dd, ²J(P,P)_c = 26 Hz, ²J(P,P)_t = 250 Hz, 1 P), 66.87 (dd, ²J(P,P)_c = 39 Hz, ²J(P,P)_c = 26 Hz, 1 P). Anal. Calcd for C₅₁H₅₄B₉P₃Ru: C, 63.92; H, 5.68. Found: C, 63.11; H, 5.86.

Synthesis of [RuH(nHPPh)(PPh₃)₂] (8). To 20 mL of ethanol solution containing 75 mg (0.191 mmol) of [NMe₄]-[nHPPh] was added [Ru(AcO)H(PPh₃)₃] (184 mg, 0.191 mmol), and the mixture was refluxed for 2 h. A yellow solid precipitated. The solution was cooled at room temperature. The solid was filtered off, washed with three portions (5 mL) of ethanol, and dried. Yield: 156 mg (83%). FTIR (KBr): ν_{\max} (B–H) = 2600, 2565, 2502 cm⁻¹, ν_{\max} (Ru–H) = 2000 cm⁻¹. ¹H FTNMR (300 MHz, CDCl₃, 25 °C, TMS): δ -13.80 (br, 1 H, RuH), -6.95 (br, 1 H, BHRu), -3.10 (br, 1 H, BHB), -2.10 (tetrap, ¹J(H,B) = 106 Hz, 1 H, BHRu), 6.39–7.53 (m, 40 H, C_{aryl}-H). ¹¹B

FTNMR (128 MHz, CDCl₃, 25 °C, BF₃·Et₂O): δ 6.84 (1 B), -13.91 (3 B), -15.82 (d, $^1J(\text{B,H}) = 106$ Hz, 1 B), -19.19 (d, $^1J(\text{B,H}) = 151$ Hz, 1 B), -26.93 (1 B), -28.43 (1 B), -34.79 (1 B). $^{31}\text{P}\{^1\text{H}\}$ FTNMR (101 MHz, CDCl₃, 25 °C, H₃PO₄, 85%): δ 32.32 (dd, $^2J(\text{P,P})_c = 41$ Hz, $^2J(\text{P,P})_t = 249$ Hz, 1 P), 53.12 (dd, $^2J(\text{P,P})_c = 27$ Hz, $^2J(\text{P,P})_t = 249$ Hz, 1 P), 66.30 (dd, $^2J(\text{P,P})_c = 41$ Hz, $^1J(\text{P,P})_c = 27$ Hz, 1 P). Anal. Calcd for C₅₀H₅₂B₉P₃Ru: C, 63.60; H, 5.55. Found: C, 63.05; H, 5.40.

Synthesis of [RuH(nPhPPH)(PPh₃)₂] (9). To 20 mL of ethanol containing 80 mg (0.126 mmol) of [NBu₄][nPhPPH] was added [Ru(AcO)H(PPh₃)₃] (119 mg, 0.126 mmol), the mixture was refluxed for 8.5 h, and a yellow solid precipitated. The solid was filtered while warm, washed with three portions (5 mL) of ethanol, and dried. Yield: 61 mg (48%). FTIR (KBr): ν_{max} (B-H) = 2565, 2558, 2530 cm⁻¹, ν_{max} (Ru-H) = 1982 cm⁻¹. $^1\text{H}\{^{11}\text{B}\}$ FTNMR (300 MHz, CD₂Cl₂, 25 °C, TMS): δ -13.90 (m, 1 H, RuH), -6.75 (d, $^2J(\text{H,P}) = 30$ Hz, 1 H, BHRu), -2.40 (s, 1 H, BHB), -1.80 (s, 1 H, BHRu), 6.72-7.53 (m, 45 H, C_{aryl}-H). ^1H FTNMR (300 MHz, CD₂Cl₂, 25 °C, TMS): δ -13.90 (br, 1 H, RuH), -6.75 (br, 1 H, BHRu), -2.40 (br, 1 H, BHB), -1.80 (tetrap, $^1J(\text{H,B}) = 106$ Hz, 1 H, BHRu), 6.72-7.53 (m, 45 H, C_{aryl}-H). ^{11}B FTNMR (96 MHz, CD₂Cl₂, 25 °C, BF₃·Et₂O): δ 3.7 (1 B), -13.3 (2 B), -18.0 (d, $^1J(\text{B,H}) = 106$ Hz, 1 B), -20.9 (d, $^1J(\text{B,H}) = 125$ Hz, 1 B), -29.4 (3 B), -37.0 (1 B). $^{31}\text{P}\{^1\text{H}\}$ FTNMR (121 MHz, CD₂Cl₂, 25 °C, H₃PO₄, 85%): δ 42.67 (dd, $^2J(\text{P,P})_c = 39$ Hz, $^2J(\text{P,P})_t = 248$ Hz, 1 P), 52.19 (dd, $^2J(\text{P,P})_c = 26$ Hz, $^2J(\text{P,P})_t = 248$ Hz, 1 P), 65.41 (dd, $^2J(\text{P,P})_c = 39$ Hz, $^2J(\text{P,P})_c = 26$ Hz, 1 P). Anal. Calcd for C₅₆H₅₆B₉P₃Ru: C, 65.92; H, 5.53. Found: C, 65.17; H, 5.49.

Synthesis of [RuCl(nMePET)(PPh₃)₂] (10). To 15 mL of ethanol solution containing 75 mg (0.157 mmol) of [NBu₄][nMePET] was added [RuCl₂(PPh₃)₃] (150 mg, 0.157 mmol), and the mixture was refluxed for 3 h. A dark orange solution was formed. The solution was concentrated to 5 mL and cooled at 0 °C. A dark red solid precipitated. The solid was filtered off and recrystallized from chloroform/heptane (1:1). Yield: 60 mg (43%). FTIR (KBr): ν_{max} (B-H) = 2572 cm⁻¹. ^1H FTNMR (300 MHz, CDCl₃, 25 °C, TMS): δ -15.20 (br, 1 H, BHRu), -4.05 (br, 1 H, BHRu), -3.11 (br, 1 H, BHB), 0.73 (m, 3 H, CH₃), 1.08 (s, 3 H, CH₃), 1.28 (m, 3 H, CH₃), 2.46 (m, 4 H, CH₂), 6.98-7.71 (m, 30 H, C_{aryl}-H). $^{11}\text{B}\{^1\text{H}\}$ FTNMR (96 MHz, CDCl₃, 25 °C, BF₃·Et₂O): δ 3.60 (1 B), -10.70 (1 B), -15.20 (2 B), -19.70 (1 B), -25.20 (1 B), -32.80 (2 B), -37.40 (1 B). $^{31}\text{P}\{^1\text{H}\}$ FTNMR (121 MHz, CDCl₃, 25 °C, H₃PO₄, 85%): δ 16.56 (dd, $^2J(\text{P,P})_c = 34$ Hz, $^2J(\text{P,P})_t = 295$ Hz, 1 P), 23.98 (dd, $^2J(\text{P,P})_c = 26$ Hz, $^2J(\text{P,P})_t = 295$ Hz, 1 P), 53.28 (dd, $^2J(\text{P,P})_c = 34$ Hz, $^2J(\text{P,P})_c = 26$ Hz, 1 P). Anal. Calcd for C₄₃H₅₃B₉P₃ClRu: C, 57.60; H, 5.96. Found: C, 56.98; H, 5.83.

X-ray Structure Determination of [RuCl(nMePPh)(PPh₃)₂] (1). Single-crystal data collection was performed at ambient temperature with a Rigaku AFC5S diffractometer using monochromatic Mo K α radiation ($\lambda = 0.71096$ Å). The unit cell parameters were determined by least-squares refinements of 25 carefully centered reflections ($22^\circ < 2\theta < 27^\circ$). The data obtained were corrected for Lorentz and polarization effects and for dispersion. An empirical absorption correction (ψ scan) was also applied. A total of 9430 reflections was collected by the $\omega/2\theta$ scan mode ($2\theta_{\text{max}} = 50^\circ$), giving 8917 unique reflections ($R_{\text{int}} = 0.037$). Of those, 5219 were considered observed according to the criteria $I > 3\sigma(I)$. The three check reflections monitored after every 150 reflections showed no decay during the course of the data collection. Crystallographic data are presented in Table 1.

The structure was solved by direct methods using MITRIL.¹⁷ Least-squares refinements and all subsequent calculations were performed by using the TEXSAN crystallographic software package,¹⁸ which minimized the function $\sum w(\Delta F)^2$ where $1/w = \sigma^2(F_o)$. Refinement of all non-hydrogen atoms with

anisotropic temperature factors, BH hydrogen atoms with fixed isotropic temperature parameters, and CH hydrogen atoms by inclusion in calculated positions with fixed isotropic temperature factors [$U(\text{H})$ equal to $1.2 \times U$ of the host atom; C-H = 0.95 Å] reduced the R value to 0.041 ($R_w = 0.056$) for 616 parameters. Neutral atomic scattering factors were those included in the program. The figure was plotted with ORTEP.¹⁹

X-ray Structure Determination of [RuCl(nMePPh)(EtOH)(PPh₃)₂]-0.64(Me)₂CO (2). Single-crystal data collection for **2** was performed at ambient temperature on a Rigaku AFC5S diffractometer. A total of 11 713 reflections was collected by the $\omega/2\theta$ scan mode ($2\theta_{\text{max}} = 50^\circ$), giving 11 247 unique reflections ($R_{\text{int}} = 0.048$). Of those, 6839 were considered observed according to the criterion $I > 2\sigma(I)$. The three check reflections monitored after every 150 reflections showed no systematic variation during the data collection. Crystallographic data are presented in Table 1.

The structure was solved by direct methods by using MITRIL.¹⁷ Least-squares refinements and all subsequent calculations were performed by using the XTAL3.2 program system,²⁰ which minimized the function $\sum w(\Delta F)^2$ [$1/w = \sigma^2(F_o)$]. The asymmetric unit of the structure contains two complex units and disordered solvent molecules. The ethanol molecule coordinated to Ru(1) is disordered, with the ethyl group assuming two orientations (occupancy: 0.50). Refinement of all non-hydrogen atoms of the complex units revealed several residual maxima of 0.5-1.0 eÅ⁻³ in large cavities between the bulky complex units. We assumed that the maxima belonged to disordered acetone molecules. Refinement of site occupation parameters of the acetone molecule did not converge well, but gave values near to 0.5 for two close acetone molecules {O(4)-C(96) and O(5)-C(99)} and 0.28(3) for the acetone molecule {O(3)-C(93)} across 1/2, 1/2, 1/2. The site occupation parameters were fixed for the disordered groups to 0.50 and 0.28 and not refined in the final refinement cycles. The metal ions, phosphorus atoms, coordinated oxygen atoms, and non-hydrogen atoms of the carborane cage were refined with anisotropic displacement parameters in the final refinements. The methyl groups bonded to the cage, and the phenyl groups and the acetone groups were refined as rigid groups with the isotropic U values for the hole group. The hydrogen atoms of the ethyl group of the ethanol molecule bonded to Ru(2), and the hydrogen atoms of the carborane cage, except H(10B) and H(30B), were placed at their calculated positions (C-H = 0.95, B-H = 1.10 Å and $U(\text{H})$ equal to $1.2 \times U$ of the host atom). Approximate positions of H(10B) and H(30B) were found from the ΔF map and were not refined. Hydrogen atoms of the disordered groups and OH hydrogen atoms were not positioned. The final R value was 0.071 ($R_w = 0.077$). Neutral atomic scattering factors were those included in the programs. The figures were plotted with XTAL-ORTEP.

Acknowledgment. This work was supported, in part, by Grant QFN92-4313 of the CIRIT. R.K. is grateful to Oskar Öflunds Stiftelse for a grant.

Supporting Information Available: Tables of X-ray experiment details, non-hydrogen and hydrogen positional and isotropic displacement parameters, anisotropic parameters, and interatomic distances and angles for **1** and **2** (37 pages). Ordering information is given on any current masthead page.

OM9509002

(17) Gilmore, C. J. *J. Appl. Crystallogr.* **1982**, *17*, 42.

(18) TEXSAN-TEXRAY: Single Crystal Structure Analysis Package, Version 5.0; Molecular Structure Corporation: The Woodlands, TX, 1989.

(19) Johnson, C. K. *ORTEP-II, Report ORNL-5138*; Oak Ridge National Laboratory: Oak Ridge, TN, 1976.

(20) Hall, S. R., Flack, H. D., Stewart, J. M., Eds. *Xtal 3.2 User's Guide*, Universities of Western Australia, Australia, and Maryland, 1992.